

## PHASE DIAGRAM OF THE SYSTEM NaF–SnF<sub>2</sub>

V. Dvořák<sup>1</sup>, V. Danielik<sup>2</sup>, O. Matal<sup>3</sup>, Marta Chrenková<sup>4</sup> and M. Boca<sup>4\*</sup>

<sup>1</sup>Department of Power Engineering, Faculty of Mechanical Engineering, Brno University of Technology, Technická 2896/2  
616 69 Brno, Czech Republic

<sup>2</sup>Department of Inorganic Technology, Faculty of Chemical and Food Technology, Slovak University of Technology  
Radlinského 9, 812 37 Bratislava, Slovakia

<sup>3</sup>ENERGOVYZKUM, Ltd., Božetěchova 17, 61200 Brno, Czech Republic

<sup>4</sup>Institute of Inorganic Chemistry, Slovak Academy of Sciences, Dúbravská cesta 9, 845 36 Bratislava, Slovakia

The phase diagram of the binary system NaF–SnF<sub>2</sub> was determined by using the thermal analysis method. In addition to the crystallisation fields of pure components the formation of three other crystallisation fields was observed and these were attributed to the compounds: NaF·2SnF<sub>2</sub>, NaF·SnF<sub>2</sub> and 2NaF·SnF<sub>2</sub>. The coordinates of the four eutectic points are:

$e_1$ : 70 mol% NaF, 30 mol% SnF<sub>2</sub> and 255°C

$e_2$ : 58 mol% NaF, 42 mol% SnF<sub>2</sub> and 238°C

$e_3$ : 44 mol% NaF, 56 mol% SnF<sub>2</sub> and 246°C

$e_4$ : 18 mol% NaF, 82 mol% SnF<sub>2</sub> and 191°C

The model independent on the real structure of the melt was applied for the calculation of phase diagram comprising the calculation of excess molar Gibbs energy of mixing. The probable inaccuracy in the calculated phase diagram is  $\sigma=2.0^\circ\text{C}$ . XRD analysis of solidified mixtures was performed in order to confirm the formation of expected compounds.

**Keywords:** excess molar Gibbs energy of mixing, phase diagram, thermal analysis, tin fluoride

### Introduction

The most favourable variant of the transmutor in nuclear power plants seems to be a three circulating loops concept with homogeneous core configuration in the primary one [1, 2]. The molten fluorides are considered as the primary coolant and the nuclear fuel carrier, simultaneously. Molten fluoride salts are also considered as the coolant for the secondary circulating loop [3]. This loop ensures heat transport between the primary and the tertiary circulating loop, which operate on the Rankine–Clausius's or the Brayton's cycle principles. A lack of information about the properties of candidate fluoride salt coolants (e.g. melting temperature, specific heat capacity, viscosity, etc.) is a reason for their research.

The chemical stability of the system and low melting temperature, in the range of operational temperatures, belong among basic coolant requirements. The condition of the low melting temperature is met also in the SnF<sub>2</sub>–NaF system. The criterion of the chemical stability can be deduced from the phase diagram of considered system. The equilibrium diagram of this system was reported in [4]. Authors reported the formation of four congruently melting compounds

at NaF–SnF<sub>2</sub> molar ratio 6:1, 2:1, 1:1, 1:2 with the melting points of 279, 273, 265 and 299°C, respectively. However, only two compounds were identified by XRD patterns; NaSn<sub>2</sub>F<sub>5</sub> and NaSnF<sub>3</sub>, respectively.

In the present work the phase diagram of the binary system NaF–SnF<sub>2</sub> was determined by using of thermal analysis and the subsequent coupled analysis of thermodynamic and equilibrium phase diagram data. The solid phases obtained from the quenched melts of mixtures of varying composition were analysed by X-ray powder diffraction.

### Experimental

For the preparation of samples the following chemicals were used: NaF (Merck, 99.5%), SnF<sub>2</sub> (Aldrich, 99.0%), NaCl (Fluka, 99.5%), and NaNO<sub>3</sub> (Lachema, 99.8%). NaF was dried at 600°C for 2 h and SnF<sub>2</sub> was dried in vacuum oven at 130°C for one day. Handling of all salts was done in a glove box under dry nitrogen atmosphere (Messer, 99.990%).

The temperatures of individual phase transitions (primary and eutectic crystallization) were determined by means of thermal analysis, recording the cooling and heating curves of the investigated mix-

\* Author for correspondence: uachboca@savba.sk

tures. The platinum crucible with the sample ( $10.000 \pm 0.001$  g) was placed into the preheated resistance furnace with a controlled Ar atmosphere (Messer, 99.996%) and adjustable cooling rate that was controlled by Clasic Clare 4.0 regulator (Czech Republic). The heating and cooling rates were 5 and  $2^{\circ}\text{C min}^{-1}$ , respectively. The temperature was measured by using a Pt–PtRh10 thermocouple calibrated to the melting points of NaCl and NaNO<sub>3</sub>. The thermocouple was connected to the multimeter Keithley 2700 DMM. The measured transition temperatures were reproducible within  $\pm 1^{\circ}\text{C}$  and they are summarised in Table 1.

**Table 1** The temperatures of primary ( $t_{\text{PC}}/^{\circ}\text{C}$ ) and eutectic ( $t_{\text{eut}}/^{\circ}\text{C}$ ) crystallization in the system NaF–SnF<sub>2</sub> together with the data published by Donaldson *et al.* [4]

$x(\text{SnF}_2)$	$t_{\text{PC,exp}}/^{\circ}\text{C}$	$t_{\text{PC,cal}}/^{\circ}\text{C}$	$\Delta t/^{\circ}\text{C}$	$t_{\text{eut}}/^{\circ}\text{C}$	$t/^{\circ}\text{C}$ [4]
1	213	213			219.5
0.95	210.5	210.64	0.14		
0.9	208	205.49	-2.51		212
0.85	201	197.42	-3.58	187	
0.83					200
0.8	211	211.93	0.93	193	215
0.78	233	231.41	-1.59		
0.75	257	256.46	-0.54		289
0.7	283	282.75	-0.25	191	
0.667	288	288.00	0		299
0.63	279	281.87	2.87		
0.61					253
0.6					250
0.57					253
0.55	254	250.75	-3.25		261
0.5	260	260	0		265
0.45	250	251.5	1.5		263
0.42					264
0.4	248	245.3	-2.7		
0.35	259	259.04	0.04		273
0.333	260	260.00	0		
0.3	259	255.42	-3.58		268
0.28					259
0.25	403		-	256	271
		371.61	31.39*		
0.2	508	509.08	1.08	254	278
15					276
10					259
0	996	996			

\*This term is excluded from the calculation of the standard deviation

X-ray powder patterns of samples were collected on Stoe Stadi P transmission diffractometer equipped with a curved Ge (111) monochromator placed in the primary beam and a linear PSD. In order to achieve a better resolution CoK<sub>α</sub> radiation was used. The records were taken in the  $2\theta$  range of  $7\text{--}70^{\circ}$  at room temperature each for 2 h. Identification of the present phases was done using the PDF-2 International Centre for Diffraction Data database [5].

## Data processing

### The calculation of the phase diagram

The calculation of the phase diagrams of condensed systems using the coupled analysis of the thermodynamic and phase diagram data is based on the solution of a set of equations of the following type [6]

$$\Delta_{\text{fus}}G_i^0(T) + RT \ln \frac{a_{\text{l},i}(T)}{a_{\text{s},i}(T)} = 0 \quad (1)$$

where  $\Delta_{\text{fus}}G_i^0$  is the standard molar Gibbs energy of fusion of the component  $i$  at the temperature  $T$ ,  $R$  is the gas constant, and  $a_{\text{s},i}(T)$  and  $a_{\text{l},i}(T)$  are the activities of component  $i$  in the solid and liquid phase at the temperature  $T$ , respectively. For  $T \equiv T_{\text{pc},i}$  and assuming  $\Delta C_{\text{p,s},i} = 0$  and the immiscibility of components in the solid phase ( $a_{\text{s},i} = 1$ ), for the thermodynamic temperature of primary crystallization of the component  $i$  one can obtain

$$T_{\text{pc},i} = \frac{\Delta_{\text{fus}}H_i^0 + RT_{\text{pc},i} \ln \gamma_{\text{l},i}}{\Delta_{\text{fus}}S_i^0 - R \ln x_{\text{l},i}} \quad (2)$$

where  $\Delta_{\text{fus}}H_i^0$  and  $\Delta_{\text{fus}}S_i^0$  is the standard enthalpy and standard entropy of fusion, respectively,  $x_{\text{l},i}$  and  $\gamma_{\text{l},i}$  is the mole fraction and the activity coefficient of component  $i$ , respectively. The activity coefficients can be calculated from the molar excess Gibbs energy of mixing

$$RT_{\text{pc},i} \ln \gamma_{\text{l},i} = \left[ \frac{\partial(n\Delta G_{\text{l}}^{\text{E}})}{\partial n_i} \right]_{T,p,n_{j \neq i}} \quad (3)$$

where  $n_i$  is the amount of component  $i$  and  $n$  is the total amount of all components.

The molar excess Gibbs energy of mixing in the liquid phase in the binary systems can be described by the following general equation:

$$\Delta G_{\text{bin}}^{\text{E}} = \sum_j x_1 x_2^j G_j \quad (4)$$

It is assumed that in the measured temperature range the molar excess Gibbs energy of mixing is independent on temperature.

*Binary system with a compound in solid-state*

Let us consider the system AX–AY, in which a compound  $m\text{AX}\cdot n\text{AY}$  is formed in the solid-state. According to [7] this compound can be written as  $(\text{AX})_p \cdot (\text{AY})_q$  where

$$p = \frac{m}{m+n}, q = \frac{n}{m+n} \quad (5)$$

It is obvious that the compound  $(\text{AX})_p \cdot (\text{AY})_q$  is formed from 1 mole of the melt and the Gibbs energy of fusion of  $(\text{AX})_p \cdot (\text{AY})_q$  equals to

$$\Delta_{\text{fus}}G^0((\text{AX})_p \cdot (\text{AY})_q) = \frac{\Delta_{\text{fus}}G^0(m\text{AX}\cdot n\text{AY})}{m+n} \quad (6)$$

The model is described in details in [8].

**Results and discussion**

The coupled thermodynamic analysis, i.e. the calculation of the coefficients  $G_j$  in the Eq. (4) has been performed using multiple linear regression analysis omitting the statistically non-important terms in the excess molar Gibbs energy of mixing on the 0.99 confidence level according to the Student test. As the optimising criterion for the best fit between the experimental and calculated temperatures of primary crystallisation the following condition was used for all measured points

$$\sum_n (T_{\text{pc,exp,n}} - T_{\text{pc,calc,n}})^2 = \min \quad (7)$$

The values of the enthalpy of fusion of individual components used in the calculation are summarised in Table 2. However, no data on the enthalpy of fusion of the phases corresponding to the composition NaF–SnF<sub>2</sub> 2:1, 1:1 and 1:2 were found in the literature. It was estimated that the respective mixtures correspond to the following compounds Na<sub>2</sub>SnF<sub>4</sub>, NaSnF<sub>3</sub> and NaSn<sub>2</sub>F<sub>5</sub>, respectively. In the calculation of the enthalpy of fusion of these phases it was assumed that the entropy of fusion of the additive compounds is approximately given by the sum of entropies of fusion of the respective components [7], e.g.:

$$\Delta_{\text{fus}}S(\text{NaSn}_2\text{F}_5) = \Delta_{\text{fus}}S(\text{NaF}) + 2\Delta_{\text{fus}}S(\text{SnF}_2) \quad (8)$$

Coefficients of the composition dependence of the molar excess Gibbs energy of mixing (Eq. (4), where subscripts 1 and 2 represent SnF<sub>2</sub> and NaF, respectively, are listed in Table 3. The standard deviation of the measured and calculated temperatures of primary crystallization is  $\sigma=2.0^\circ\text{C}$ .

The calculated phase diagram of the system NaF–SnF<sub>2</sub> from the experimental data is shown in Fig. 1 together with data by Donaldson *et al.* [4]. The formation of three congruently melting compounds of

**Table 2** Temperatures and enthalpies of fusion of compounds used for the phase diagram calculation

Compound	$\Delta_{\text{fus}}H^0 / \text{kJ mol}^{-1}$	$T_{\text{fus}} / \text{K}$	Ref.
NaF	33.137	1269	[9]
SnF <sub>2</sub>	10.503	486	[10]
NaSn <sub>2</sub> F <sub>5</sub>	38.897	561	[this work – Eq. (8)]
NaSnF <sub>3</sub>	25.437	533	[this work – like Eq. (8)]
Na <sub>2</sub> SnF <sub>4</sub>	39.355	533	[this work – like Eq. (8)]

**Table 3** Coefficients of the molar excess Gibbs energy of the system NaF–SnF<sub>2</sub>

Coefficient	Value/kJ mol <sup>-1</sup>
$G_1$	$-(64.2 \pm 4.3)$
$G_2$	$-(177.7 \pm 61.3)$
$G_3$	$(373.4 \pm 112.4)$
$G_4$	$-(317.3 \pm 67.9)$

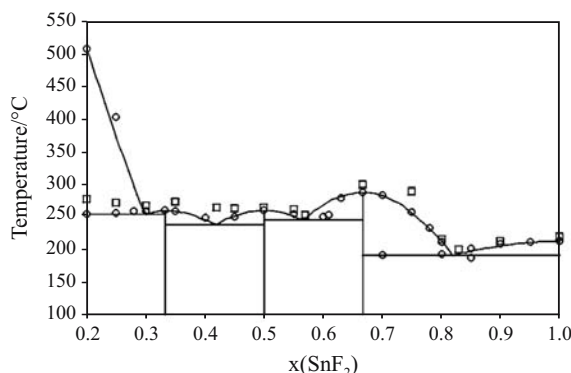


**Fig. 1** Phase diagram of the system NaF–SnF<sub>2</sub>. ○ – this work (experiment); full line – calculated □ – Donaldson *et al.* [4]

the composition NaF·2SnF<sub>2</sub>, NaF·SnF<sub>2</sub> and 2NaF·SnF<sub>2</sub> was confirmed, similarly as in [4]. Their respective melting points are 288°C (299°C [4]), 260°C (265°C [4]) and 260°C (273°C [4]). The existence of the compound 6NaF·SnF<sub>2</sub>, proposed by Donaldson *et al.* [4], seems to be unlikely. The part of the system with SnF<sub>2</sub> content lower than 30 mol% is difficult to measure as it seems to be ‘unstable’. The temperature necessary for melting the system of this composition is too high. Thus SnF<sub>2</sub> or SnF<sub>2</sub>-containing compounds evaporate or decompose and composition of the melt changes. Significant differences between temperatures of primary crystallisation reported here and reported in [4] can be found in Table 1 for composition below 25 mol% of SnF<sub>2</sub>. It can be explained by the fact that temperatures that Donaldson *et al.* [4] has attributed to primary crystallisation temperatures are, indeed, eutectic tempera-

tures. The last difference can be found in the melting point of pure  $\text{SnF}_2$  that is 213°C [10, 11] in comparison with 219°C by Donaldson *et al.* [4].

The calculated coordinates of the four eutectic points are:

- $e_1$ : 70 mol% NaF, 30 mol%  $\text{SnF}_2$  and 255°C
- $e_2$ : 58 mol% NaF, 42 mol%  $\text{SnF}_2$  and 238°C
- $e_3$ : 44 mol% NaF, 56 mol%  $\text{SnF}_2$  and 246°C
- $e_4$ : 18 mol% NaF, 82 mol%  $\text{SnF}_2$  and 191°C

The course of the excess molar Gibbs energy in this system is shown in Fig. 2. From Fig. 2 it follows that there is a strong exothermic reaction in the whole concentration region. This type of deviation from the additivity can be explained by the formation of complex anions  $[\text{Sn}_x\text{F}_y]^{y-2x}$  in the melts.

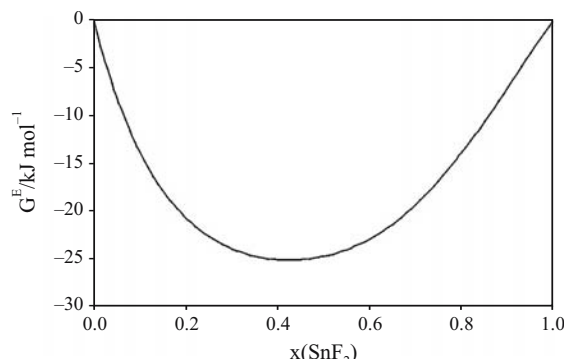


**Fig. 2** Excess molar Gibbs energy of mixing in the system NaF– $\text{SnF}_2$

Identification of the products at compositions  $\text{NaF}\cdot 2\text{SnF}_2$ ,  $\text{NaF}\cdot \text{SnF}_2$  and  $2\text{NaF}\cdot \text{SnF}_2$  met with some difficulties. The XRD pattern of the powdered quenched sample of the composition of  $\text{NaF}\cdot 2\text{SnF}_2$  perfectly fits to the XRD pattern calculated from the known structure of the compound  $\text{NaSn}_2\text{F}_5$  (PDF card No. 71-1961) [12]. Data provided by Donaldson [13] for this compound, however, significantly disagree in intensities with the data retrieved from the structure [12]. XRD pattern of the sample with composition  $\text{NaF}\cdot \text{SnF}_2$  exhibit completely different structure as data reported for  $\text{NaSnF}_3$  by Donaldson [13] (PDF card No. 16-788) and do not match any XRD pattern of known relevant compounds. The authors [13] reported the preparation of this compound from water solution as pure crystalline compound. Single crystal structural identification should be done in order to make unambiguous conclusion on the existing phases. However, this was not the aim of this work. On the other hand, there is also possibility that  $\text{NaSnF}_3$  does not exist in the solid-state in the measured temperature range. The similar behaviour was described in the NaF– $\text{Na}_2\text{SO}_4$  system [14].

XRD pattern of the sample with composition  $2\text{NaF}\cdot \text{SnF}_2$  corresponding to the compound  $\text{Na}_2\text{SnF}_4$

cannot be confirmed as no data for this compound are known. The formation of the  $\text{Na}_4\text{Sn}_3\text{F}_{10}$  [15], that was prepared from water solutions, can be expected at the composition  $4\text{NaF}\cdot 3\text{SnF}_2$ , however this was not observed in the samples prepared from molten reactants. At this composition the XRD pattern showed the same structure as XRD pattern for composition  $\text{NaF}\cdot \text{SnF}_2$ . Samples with  $\text{SnF}_2$  content lower than 33 mol% showed NaF diffraction in their XRD patterns.

## Acknowledgements

Slovak Grant Agencies (VEGA-2/6179/26, VEGA-1/2108/05) are acknowledged for financial support.

## References

- 1 Ch. D. Bowman, Accelerator-Driven Systems For Nuclear Waste Transmutation. The ADNA Corporation, Accelerator-Driven Neutron Applications, Los Alamos, New Mexico 87544, Annu. Rev. Nucl. Part. Sci. 1998.
- 2 H. G. MacPherson, The Molten Salt Reactor Adventure. Nuclear Science and Engineering. Oak Ridge 1985.
- 3 L. M. Toth, U. Gat, G. D. Del Cul, S. Dai and D. F. Williams, Review of ORNL's MSR Technology and Status. Oak Ridge National Laboratory, Oak Ridge, TN 37381, 1995.
- 4 J. D. Donaldson, J. D. O'Donogue and R. Oteng, J. Chem. Soc., (1965) 3876.
- 5 PDF-2 Database 2003, International Centre for Diffraction Data.
- 6 B. Foosnaes, T. Østvold and H. Øye, Acta Chem. Scand., A32 (1978) 773.
- 7 M. Chrenková, V. Danielík, B. Kubíková and V. Danek, Calphad, 27 (2003) 19.
- 8 M. Boca, V. Danielík, Z. Ivanova, E. Mikšíkova and B. Kubíkova, J. Therm. Anal. Cal. OnlineFirst: DOI: 10.1007/s10973-006-7700-5.
- 9 Chase Malcolm, NIST-JANAF, Thermochemical Tables – Fourth Edition, J. Phys. Chem. Ref. Data, Mono. No. 9, 1998.
- 10 O. Knacke, O. Kubaschewski and K. Hesselman, Thermochemical Properties of Inorganic Substances, 2<sup>nd</sup> Ed., Springer-Verlag, Berlin 1991, pp.1114–2412.
- 11 D. R. Lide, CRC Handbook of Chemistry and Physics, 82<sup>nd</sup> Edition, CRC Press, 2001.
- 12 R. R. McDonald, A. C. Larson and D. T. Cromer, Acta Crystallogr., 17 (1964) 1104.
- 13 J. D. Donaldson and J. D. O'Donoghue, J. Chem. Soc., (1964) 271.
- 14 V. Danielík, J. Gabčová and P. Fellner, Chem. Pap., 53 (1999) 233.
- 15 G. Bergerhoff and L. Goost, Acta Crystallogr., B26 (1970) 19.

Received: December 29, 2006

Accepted: May 8, 2007

DOI: 10.1007/s10973-006-8320-9